Journal Name

ARTICLE TYPE

Cite this: DOI: 10.1039/xxxxxxxxxx

The structure of liquid water beyond the first hydration shell†

Andres Henao,[a,b] Sebastian Busch,[c] Elvira Guàrdia,[b] Josep Lluis Tamarit,[a] and Luis Carlos Pardo*[a]

Received Date
Accepted Date

DOI: 10.1039/xxxxxxxxxx

www.rsc.org/journalname

There is to date a general consensus on the structure of the first coordination shells of liquid water, namely a tetrahedral short range order of the molecules. In contrast, little is known about the structure at longer distances and the influence of the tetrahedral molecular arrangement of the first shells on the order at these length scales. An expansion of the distance dependent excess entropy is used in this contribution to find out which molecular arrangements are important at each distance range. This was done by splitting the excess entropy into two parts: one connected to the relative *position* of two molecules, and the other one related to their relative *orientation*. A transition between two previously unknown regimes in liquid water is identified at a distance of about ∼6 Å: from a predominantly orientational order at shorter distances to a regime at larger distances of up to ∼9 Å where the order is predominantly positional and molecules are distributed with the same tetrahedral symmetry as the very first molecules.

1 Introduction

The relative position and orientation of molecules in liquid water within the first hydration shell have been intensively studied by many scientists. Some alternative visions of the structure of liquid water seemed to diverge from the classical tetrahedral coordination description[1–6]: some of them propose a chain and ring structure[7], others a two-state model for liquid water[8–10], or the existence of trigonal configurations in liquid water[4,5]. It appears now that it is possible to conciliate some of these new descriptions with the classical one. According to this unifying view, water is tetrahedrally coordinated, but there is some asymmetry in the strength of hydrogen bonds due to the relative orientation of the two neighbouring water molecules[6,11].

Molecular ordering in liquid water at short distances is thus affected by highly directional hydrogen bonding and steric repulsion. Both effects are important close to a given central molecule of water, but it remains unclear how these two effects affect two water molecules which are far away from each other. In other words, little attention has been paid on how this particular arrangement affects the structure of water molecules at distances larger than a few molecular radii. The work of Liu et al.[12] is an exception. They found angular correlations persisting on a length scale of ∼40 Å using Density Functional Theory. In that work it seemed that the special molecular arrangements are not correlated to the local density probed by the Oxygen-Oxygen partial radial distribution function $g_{OO}(r)$. Higo et al. also found angular correlations in bulk water[13]. They obtained a dipole chain order for distances up to ∼10 Å.

In this contribution, the distance dependent excess entropy is used in order to characterize the structure of liquid water at distances of up to ∼9 Å. The excess entropy of a liquid is a way to quantify how different its structure is from the one of an ideal gas, thus it is defined as $S^{\text{excess}} = S^{\text{liq}} - S^{\text{gas}}$ where S^{liq} and S^{gas} are the entropies related to the liquid and the ideal gas. Since the ideal

[a] Grup de Caracterització de Materials, Departament de Física, ETSEIB, Universitat Politècnica de Catalunya, Diagonal 647, E-08028 Barcelona, Catalonia, Spain; E-mail: luis.carlos.pardo@upc.edu

[b] Grup de Simulació per Ordinador en Matèria Condensada, Departament de Física, B4-B5 Campus Nord, Universitat Politècnica de Catalunya, E-08034 Barcelona, Catalonia, Spain

[c] German Engineering Materials Science Centre (GEMS) at Heinz Maier-Leibnitz Zentrum (MLZ), Helmholtz-Zentrum Geesthacht GmbH, Lichtenbergstr. 1, 85747 Garching bei München, Germany

† Electronic Supplementary Information (ESI) available: A summary of the Information Theory approach as well as a complete set of the positional distribution functions. See DOI: 10.1039/b000000x/

gas is more disordered than the liquid, this magnitude is always negative. The calculation of the excess entropy involves the determination of the N-body correlation function that specifies the position of all the particles in the liquid.

It is possible to factorize this correlation function as a series of correlation functions with increasing complexity, involving an increasing number of particles. This factorization leads to an expression of the excess entropy that can be truncated at the two body correlation function which contains the information of both the relative position and orientation of two molecules (details can be found in the literature[14–19] and the ESI†). Even in the simple case of two-body correlations there is still the need to calculate the correlation function for 6 variables. It is therefore necessary to factorize this 6-dimensional function[19].

One way to do this factorization is to use an expansion in mutual information terms[20] which is based on the mutual information expansion of an N-dimensional Probability Density Function[21]. This expansion was employed to characterize the molecular ordering as a function of distance. The obtained distance-dependent excess entropies give access to the long distance ordering in liquid water.

The paper is organized as follows: the molecular dynamics simulation is presented first with a brief description of the calculation of the excess entropy. Details of this calculation can be found in the ESI†. Then the orientational and positional contributions to the excess entropy are described and their correlation with features in the radial distribution function is discussed.

2 Methods

2.1 Molecular dynamics simulation

Molecular Dynamics (MD) simulations were analysed in order to characterize the long range order in liquid water. The simulations were carried out using Gromacs[22] on the TIP4P/2005[23] force field as in a previous publication on the structure of water[11]. This particular model for water was chosen since it is known to be the best available to describe the structural properties of liquid water when compared with many other water models[24–26]. It is also the best model to reproduce many other experimental quantities[23] at ambient conditions such as density, isothermal compressibility, thermal expansion coefficient, heat capacity at constant pressure, heat of vaporization, static dielectric constant, self-diffusion coefficient and the melting temperature.

The time step was chosen as 1 fs since it is a rigid model, constraining the angles and bonds with the LINCS algorithm[27]. The simulation was run on 432 molecules in an NPT ensemble at the thermodynamic conditions of liquid water, $T=298$ K and $P=1$ bar using a Nose-Hoover[28] thermostat and an isotropic Parrinello-Rahman[29] barostat with coupling relaxation times of 2 ps. The cut-off was set to 9.0 Å for the van der Waals and 8.5 Å for the short-range electrostatic interactions; the particle mesh Ewald method was used beyond the electrostatic cut-off for the reciprocal space summation. 5000 snapshots of the simulation were saved for further analysis with a spacing of one picosecond.

2.2 Structure characterization by excess entropy calculation

A complete description of a liquid is possible with the N-body correlation function $g^{(N)}(\mathbf{r}^{(N)},\boldsymbol{\omega}^{(N)})$, where the position of each of the N particles is described by its vector $\mathbf{r}$ and its orientation by three angles $\boldsymbol{\omega}$. Although this correlation function describes the structure, it is of little practical use. An alternative approach to grasp the meaning of this correlation function is to describe the molecular ordering by the use of a series of hierarchical correlation functions including an increasing number of particles $g^{(2)}(\mathbf{r}^{(2)},\boldsymbol{\omega}^{(2)})$, $g^{(3)}(\mathbf{r}^{(3)},\boldsymbol{\omega}^{(3)})$ and so on. Three body correlation functions are thus regarded as corrections to two-body interactions, and this can be done for an increasing number of particles.

It is known that the two-body correlations account not only for 85%–95% of the excess entropy of simple systems (such as hard spheres or Lennard-Jones fluids) but are also able to reproduce the experimentally measured value of the excess entropy of water very well, even though water is of course not a simple Lennard-Jones liquid.[24,30] The present contribution will therefore concentrate on the two-body correlation functions $g^{(2)}(\mathbf{r}^{(2)},\boldsymbol{\omega}^{(2)})$, which will be referred to as $g(r,\Omega)$ in the following to simplify notation as detailed in the following.

Within this approximated description of the local ordering of the liquid by the pair correlation function $g(r,\Omega)$, this quantity depends on the distance r between two particles and on five angles Ω that describe their relative position and orientation. At a given distance r between particles, a new correlation function $g(\Omega|r)$ shows the probability to find a second molecule at a certain position (spherical coordinates θ_{pos}, ϕ_{pos}) and in a certain relative orientation (Euler angles θ_{ori}, ϕ_{ori} and ψ_{ori}). All these correlation functions at a given distance are normalized so that $\int g(\Omega|r)\mathrm{d}\Omega = \int \mathrm{d}\Omega$, following previous works.[30]

Figure 1 shows the definition of the angles that were used to analyse the MD trajectories: θ_{pos} and ϕ_{pos} describe the position of the second molecule with respect to the first in spherical coordinates when choosing the dipolar axis of water as z axis and the x axis perpendicular to the plane of the molecule. The Euler angles θ_{ori} and ϕ_{ori} describe the orientation of the dipolar axis of the second molecule with respect to the central one, and ψ_{ori} describes the rotation of the second water molecule around that axis.

A measure to quantify how much the correlation functions of a liquid deviate from the completely random state (the ideal gas) at a given distance is the excess entropy. Excess entropy can be split into four different parts, one related to density ($S_{\mathrm{trans}}(r)$), and three related to angular correlation functions that participate in the calculation of $S_{\mathrm{ang}}(r)$. These contributions are the following:

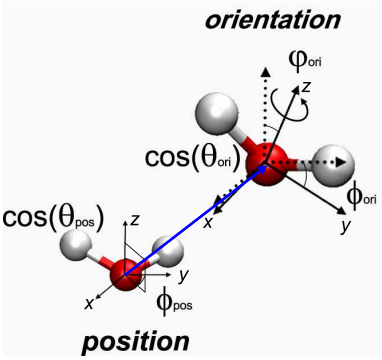

Fig. 1 (color online). Definition of axes used to calculate the positional $g(\theta_{\rm pos},\phi_{\rm pos}|r)$ and orientational $g(\theta_{\rm ori},\phi_{\rm ori},\psi_{\rm ori}|r)$ correlation functions.

1. a term associated with the molecular density at a given distance $g_{\rm OO}(r)$ with the corresponding excess entropy ,
2. a term associated with the relative position of two molecules at a given distance $g(\theta_{\rm pos},\phi_{\rm pos}|r)$ with the corresponding excess entropy $S_{\rm pos}(\theta_{\rm pos},\phi_{\rm pos}|r)$,
3. a term associated with the relative orientation of two molecules at a given distance $g(\theta_{\rm ori},\phi_{\rm ori},\psi_{\rm ori}|r)$ with the corresponding excess entropy $S_{\rm ori}(\theta_{\rm ori},\phi_{\rm ori},\psi_{\rm ori}|r)$, and finally
4. a term containing the cross-terms of positional and orientational angular variables with the corresponding excess entropy $S_{\rm pos\star ori}$.

In the following, the formulae used to calculate each of the excess entropy terms in the program ANGULA[31] are summarized, a more detailed account is given in the ESI†.

The translational component $S_{\rm trans}$ is related to the deviation of the microscopic molecular density at a given distance r from the macroscopic one, encoded in the partial radial distribution function $g_{\rm OO}(r)$:

$$S_{\rm trans}(r) := -\left[g_{\rm OO}(r)\ln\left(g_{\rm OO}(r)\right) - g_{\rm OO}(r) + 1\right] 4\pi r^2 \qquad (1)$$

The remaining three angular components $S_{\rm ang}$ contains information about how the distributions of the five angles describing the relative position and orientation of two molecules differ from the ideal gas case, and it can be calculated as (see the ESI† for details):

$$S_{\rm ang}(r) := -\frac{1}{\Omega}\int g(\Omega|r)\ln\left(g(\Omega|r)\right)\,{\rm d}\Omega \qquad (2)$$

where Ω is the integral over all five angles defining the relative position and orientation of two molecules in space. The angular excess entropy can be calculated from the 5-dimensional distribution function $g(\Omega|r)$, or using an expansion of the excess entropy related to single-angle correlation functions plus mutual information terms associated with higher order terms[21] (see the ESI† for details). When expanded only to three-angle correlations, this term can be further divided into three terms: a first one related to the position of two molecules ($S_{\rm pos}(\theta_{\rm pos},\phi_{\rm pos}|r)$),

$$S_{\rm pos}(\theta_{\rm pos},\phi_{\rm pos}|r) := -\frac{1}{\Omega_{\rm pos}}\int g\left(\theta_{\rm pos},\phi_{\rm pos}|r\right)\ln\left(g\left(\theta_{\rm pos},\phi_{\rm pos}|r\right)\right)\,{\rm d}\Omega \qquad (3)$$

a second one related to their relative orientation ($S_{\rm ori}(\theta_{\rm ori},\phi_{\rm ori},\psi_{\rm ori}|r)$)

$$S_{\rm ori}(\theta_{\rm ori},\phi_{\rm ori},\psi_{\rm ori}|r) := -\frac{1}{\Omega_{\rm ori}}\int g\left(\theta_{\rm ori},\phi_{\rm ori},\psi_{\rm ori}|r\right)\ln\left(g\left(\theta_{\rm ori},\phi_{\rm ori},\psi_{\rm ori}|r\right)\right)\,{\rm d}\Omega \qquad (4)$$

and a third one that depends on cross-terms of positional and orientational angles $S_{\rm pos\star ori}$.

$$S_{\rm pos\star ori} := S_{\rm ang} - S_{\rm pos} - S_{\rm ori} \qquad (5)$$

Where $\Omega_{\rm pos} = 4\pi$ is the integral over the angles defining the position θ_{pos} and ϕ_{pos}, and $\Omega_{\rm ori} = 8\pi^2$ is the integral over the angles defining the orientation θ_{ori}, ϕ_{ori} and ψ_{ori}. In these equations, the angular position of a second molecule at a certain distance r is encoded in the correlation function $g(\theta_{\rm pos},\phi_{\rm pos}|r)$, and their relative orientation in $g(\theta_{\rm ori},\phi_{\rm ori},\psi_{\rm ori}|r)$. The aforementioned separation is justified by analysing how strongly correlated the angular variables are, via an analysis of the mutual information between them (see the ESI† for details). This separation into purely positional and orientational contributions is only possible when the excess entropy is expanded up to the third order, for higher orders the variables are inevitably mixed.

It should be stressed that the excess entropies are obtained by an integration of their respective N-dimensional correlation functions. Just like any other order parameter, excess entropies capture only selected features of the correlation functions. In the present case, values of excess entropy close to zero correspond to a correlation function which is close to the one of an ideal gas, i. e. a flat distribution without any features. As the values of excess entropy become increasingly negative, more features appear in the correlation functions which are related to specific positions and orientations of the molecules.

3 Results and discussion

Figure 2 shows the different contributions to the excess entropy along with the radial distribution function $g_{\rm OO}(r)$. There are two contributions which yield only a very limited amount of physical insight: $S_{\rm trans}$ and $S_{\rm pos\star ori}$. For the translational excess entropy, it can readily be seen that its minima line up with extrema (minima

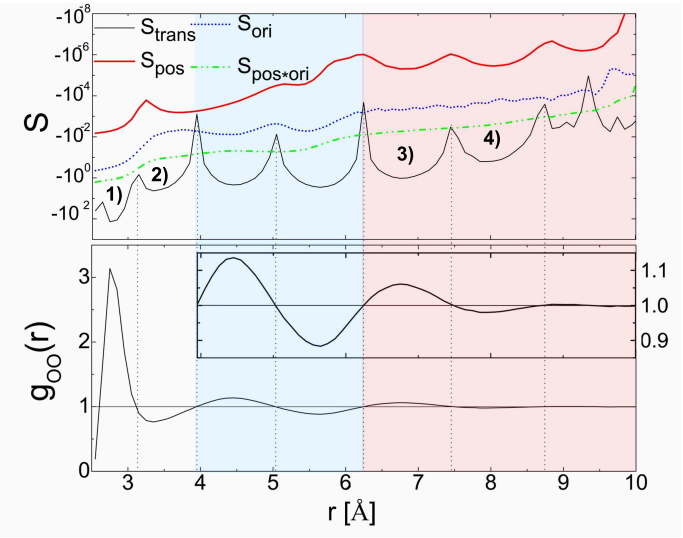

Fig. 2 (color online). Different contributions to the excess entropy S as a function of distance on a logarithmic scale. Black thin line: Absolute translational contribution $S_{\mathrm{trans}}(r)$; red thick line: positional contribution $S_{\mathrm{pos}}(r)$; blue dotted line: orientational contribution $S_{\mathrm{ori}}(r)$; green dash-dotted line: mixed positional and orientational contributions $S_{\mathrm{pos}\star\mathrm{ori}}(r)$ to the total third-order excess entropy. Also shown in the lower panel is the oxygen-oxygen radial distribution function, with a zoom in the inset to show the oscillations more clearly. The numbering is related to the shells described in the text.

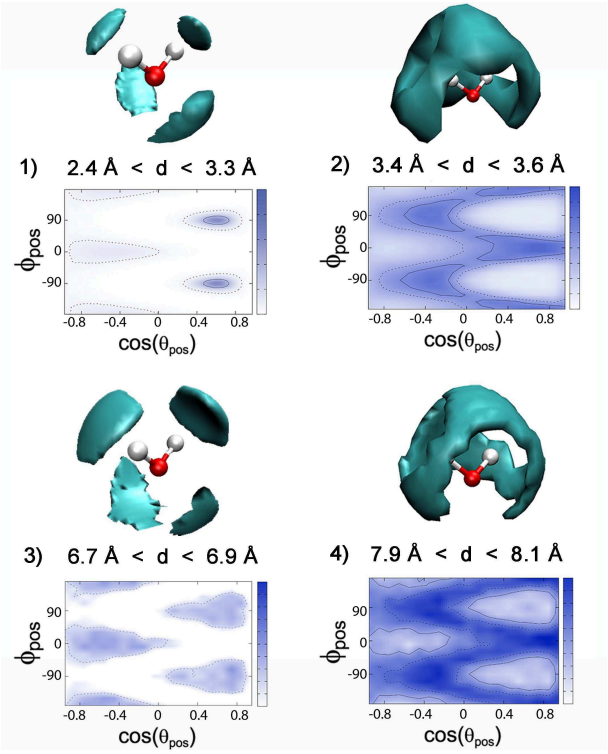

Fig. 3 (color online). Spatial density maps and distribution functions $g(\theta_{\mathrm{pos}},\phi_{\mathrm{pos}}|r)$ associated to the regions defined in figure 2: (1) 2.4-3.3 Å, (2) 3.4-3.6 Å, (3) 6.7-6.9 Å and (4) 7.9-8.1 Å.

or maxima) of $g_{\mathrm{OO}}(r)$. This correlation is not surprising due to the direct connection to the local density, cf. equation (1); whenever the density is equal to the one of the ideal gas ($g(r) = 1$), the corresponding excess entropy approaches zero. The sharp cusps of this function in the figure are caused by the representation of these small values on a logarithmic scale, S_{trans} is continuous and derivable. The contribution of the cross-term $S_{\mathrm{pos}\star\mathrm{ori}}$ (cf. equation 5) is in contrast almost featureless and does hence not provide any information.

The interesting contributions depicted in figure 2 are $S_{\mathrm{pos}}(r)$ and $S_{\mathrm{ori}}(r)$. It is worth noting that the calculation of these magnitudes does not involve the radial distribution function $g_{\mathrm{OO}}(r)$ (cf. equations 3 and 4), they are therefore *per se* independent of fluctuations in the local density. This is a very important fact since it allows to investigate if the changes in density correlate with the relative position or orientation of the molecules: Between the third and fifth node of $g_{\mathrm{OO}}(r)$, i. e. at distances between 4.0 Å and 6.2 Å, there is indeed a correlation between the value of the translational excess entropy (and thus $g_{\mathrm{OO}}(r)$) and the purely *orientational* contribution to the excess entropy $S_{\mathrm{ori}}(r)$ – the minima of both functions are located at the same distances. This can be rationalized by the well-known fact that hydrogen bonding is highly directional and, therefore, it has a big effect on the water molecules which are close together.

For longer distances, the orientational contribution is structureless and tends asymptotically to zero as the system gets more disordered. However, at those distances above 6.2 Å, it is the *positional* contribution to the excess entropy $S_{\mathrm{pos}}(r)$ which is correlated with the translational excess entropy and therefore also with $g_{\mathrm{OO}}(r)$ – both functions have the same series of minima for these distances. It is interesting to note that both, $S_{\mathrm{pos}}(r)$ and $S_{\mathrm{ori}}(r)$ exhibit a feature at ∼5.4 Å, indicating that there is a smooth transition between the two regimes: from the orientational one at distances $\lesssim$5.4 Å to the positional one at distances $\gtrsim$5.4 Å, both "active" at 5.4 Å. In the following, these two regimes will be studied in more detail.

The features of $S_{\mathrm{pos}}(r)$ correlate in the distance range between 6.2 Å and 9.0 Å with the ones of the translational excess entropy. In order to find out which molecular arrangements cause these features, the two-dimensional correlation function $g(\theta_{\mathrm{pos}},\phi_{\mathrm{pos}}|r)$ is shown in figure 3 for the distance ranges 6.7 Å$<r<$6.9 Å (in region 3) and 7.9 Å$<r<$8.1 Å (in region 4) which correspond to the positions of the minima of $S_{\mathrm{pos}}(r)$. Also plotted in the same figure are the results for the distance range 2.4 Å$<r<$3.3 Å (in region 1) and 3.4 Å$<r<$3.6 Å (in region 2). The distance range up to the first node contains roughly the first four water molecules which

form a tetrahedron, the molecules in region 2 (chosen as those around the minimum of $g_{OO}(r)$) are located in the vacancies of this first tetrahedron. For the sake of completeness, the results for all distances in steps of 0.1 Å can be found in the ESI†. The maps are well defined for the whole distance range, even up to the last minimum of $S_{pos}(r)$ at about 9.3 Å. It should be pointed out that while the number of molecules in each lobe for the first region is approximately one, so that each vertex of the tetrahedra contains one water molecule, this is not the case for region 3. The number of molecules per lobe is about 5, therefore the lobes are not representing the position of *single water molecules*, but rather the inhomogeneity of the molecular distribution in the shell. This average distribution has, as shown in figure 3, a tetrahedral symmetry.

In agreement with previous works, it can be seen that molecules continue to fill the gaps of previous hydration shells in a more or less disordered way[32–34]. To make the meaning of $g(\theta_{pos},\phi_{pos})$ more intuitive, the same information is shown in this figure also as three-dimensional Spatial Distribution Maps[35] (SDM). It is immediately visible both looking at the correlation function and the generated SDM for regions 3 and 4 that the structure is astonishingly well defined at these long distances. Even more surprising is that the structures at such long distances (maps 3 and 4) reproduce the tetrahedral structure at short distances (maps 1 and 2). The maps show unambiguously that the structures are much better defined than one might have expected from the small values of the excess entropy. Therefore, there is a correlation between an angular magnitude and both the $g_{OO}(r)$ and $S_{trans}(r)$, contrary to the results of earlier studies[12].

The features in $S_{ori}(r)$ correlate in the distance range between 4.0 Å and 6.2 Å with the ones of the translational excess entropy. In order to investigate the origin of this correlation, the orientational contribution was further separated into two independent contributions, $g(\cos(\theta_{ori}))$ and $g(\phi_{ori},\psi_{ori})$, which correspond to the angle between the two dipoles and the rotation around this axis, respectively. Their contributions to the orientational excess entropy can be calculated as (see the ESI† for details):

$$S(\cos(\theta_{ori})) = -\frac{1}{2}\int g(\cos(\theta_{ori}))\ln[g(\cos(\theta_{ori}))]\,\mathrm{d}\cos(\theta_{ori}) \quad (6)$$

$$S(\phi_{ori},\psi_{ori}) = -\frac{1}{4\pi^2}\int g(\phi_{ori},\psi_{ori})\ln[g(\phi_{ori},\psi_{ori})]\,\mathrm{d}\phi_{ori}\mathrm{d}\psi_{ori} \quad (7)$$

Figure 4 shows the values of the orientational excess entropy $S_{ori}(r)$ together with the two parts defined above. They rule the behaviour of the total orientational excess entropy S_{ori}, exhibiting all features at about the same distances for 4.0 Å$<r<$6.2 Å.

Since the angle between dipoles, and the rotation around this axis, seem to be the main contributions to orientational excess entropy, figure 4 shows the probability distribution function of the cosine of the dipolar angle as a function of the distance. It

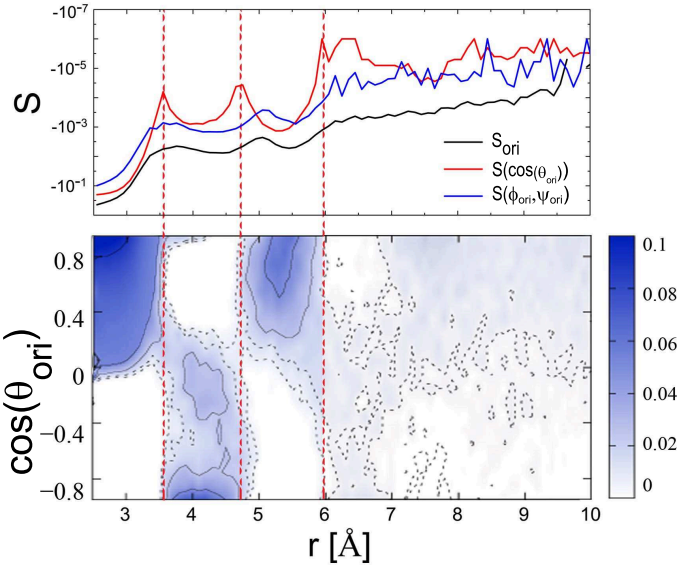

Fig. 4 (color online). Upper panel: Orientational excess entropy S_{ori} and the two independent contributions $S(\cos(\theta_{ori}))$ and $S(\phi_{ori},\psi_{ori})$ as a function of distance. Lower panel: Probability distribution function of the cosine of the angle between dipoles $\cos(\theta_{ori})$ as a function of the distance. Dashed lines serve as an eye guide to delimitate regions of maxima and minima arising from $S(\cos(\theta_{ori}))$.

shows the existence of an alternating dipole orientation starting from being parallel in the first hydration shell[11], turning to an antiparallel alignment and back to being parallel before vanishing in noise at $r\sim$6 Å. This result agrees with previous works since the spontaneously formed chain of dipoles observed here might be related to the vortices that were found to form around molecules in aqueous solution. These structures have been suggested to be important for mediating interactions between solute molecules over larger distances[13,36].

That positional correlations between molecules hold at long distances, while dipole orientations cancel out can be rationalized by the different nature of dipole interactions and steric effects: while the first are long-ranged and can cancel out at long distances, the second ones are short-ranged and are the main driving force for positioning molecules in empty spaces when going far away from the central molecule.

4 Conclusions

Excess entropy calculations allow to determine if changes in molecular ordering and in local density are correlated with the relative position or orientation of molecules. Using these functions it seems that the ordering of liquid water at distances larger than ∼4 Å is ruled for distances up to about ∼6 Å by an alternating *orientation* of water dipoles, while at distances between ∼6 Å and ∼9 Å it is the *position* of water molecules that dominates the

changes in molecular ordering. Even at distances as long as 9 Å there are "shells" which reproduce the well-known tetrahedrality of the first four water molecules. While the short-range behaviour has been observed before, i. e. that the relative orientation of water molecules is not random and that this effect is most probably driven by hydrogen bonding, the long-range behaviour was unexpected.

This special positional order could constitute a new mechanism for long-distance interactions between molecules in aqueous solution, such as for example in molecular recognition or protein-protein interactions, which would play a role together with long dipole-chains reported in the literature [13,36].

5 Acknowledgements

This work was supported by the Spanish MINECO (grants No. FIS2014-54734-P and FIS2012-39443-C02-01) and by the Government of Catalonia (grants No. 2009SGR-1003 and 2014SGR-00581).

References

1 F. H. Stillinger, *Science*, 1980, **209**, 451–457.
2 T. Head-Gordon and G. Hura, *Chem. Rev.*, 2002, **102**, 2651.
3 A. K. Soper, *Pure Appl. Chem.*, 2010, **82**, 1855.
4 R. H. Henchman and S. J. Irudayam, *The Journal of Physical Chemistry B*, 2010, **114**, 16792–16810.
5 N. Agmon, *Accounts of Chemical Research*, 2011, **45**, 63–73.
6 T. D. Kühne and R. Z. Khaliullin, *Nature Communications*, 2013, **4**, 1450.
7 P. Wernet, D. Nordlund, U. Bergmann, M. Cavalleri, M. Odelius, H. Ogasawara, L. Näslund, T. Hirsch, L. Ojamäe, P. Glatzel *et al.*, *Science*, 2004, **304**, 995–999.
8 T. Tokushima, Y. Harada, O. Takahashi, Y. Senba, H. Ohashi, L. G. Pettersson, A. Nilsson and S. Shin, *Chemical Physics Letters*, 2008, **460**, 387–400.
9 C. Huang, K. T. Wikfeldt, T. Tokushima, D. Nordlund, Y. Harada, U. Bergmann, M. Niebuhr, T. Weiss, Y. Horikawa, M. Leetmaa *et al.*, *Proceedings of the National Academy of Sciences*, 2009, **106**, 15214–15218.
10 A. Nilsson and L. G. M. Pettersson, *Chem. Phys.*, 2011, **389**, 1–34.
11 L. C. Pardo, A. Henao, S. Busch, E. Guàrdia and J. L. Tamarit, *Phys. Chem. Chem. Phys.*, 2014, **16**, 24479–24483.
12 Y. Liu and L. Wu, *J. Chem. Phys.*, 2013, **139**, 041103.
13 J. Higo, M. Sasai, H. Shirai, H. Nakamura and T. Kugimiya, *Proceedings of the National Academy of Sciences*, 2001, **98**, 5961–5964.
14 H. S. Green, *The molecular theory of fluids*, North-Holland Publishing Company Amsterdam, 1952.
15 R. Nettleton and M. Green, *The Journal of Chemical Physics*, 1958, **29**, 1365–1370.
16 T. Morita and K. Hiroike, *Progress of Theoretical Physics*, 1961, **25**, 537–578.
17 R. D. Mountain and H. J. Raveché, *The Journal of Chemical Physics*, 1971, **55**, 2250–2255.
18 D. C. Wallace, *The Journal of Chemical Physics*, 1987, **87**, 2282–2284.
19 T. Lazaridis and M. Karplus, *The Journal of Chemical Physics*, 1996, **105**, 4294–4316.
20 D. J. Huggins, *J. Chem. Phys.*, 2012, **136**, 064518.
21 H. Matsuda, *Phys. Rev. E.*, 2000, **62**, 3096–3102.
22 B. Hess, C. Kutzner, D. van der Spoel and E. Lindahl, *J. Chem. Comput.*, 2008, **4**, 435–447.
23 J. L. F. Abascal and C. Vega, *J. Chem. Phys.*, 2005, **123**, 234505.
24 J. Zielkiewicz, *The Journal of Chemical Physics*, 2005, **123**, 104501.
25 L. Pusztai, O. Pizio and S. Sokolowski, *The Journal of Chemical Physics*, 2008, **129**, 184103.
26 Z. Steinczinger and L. Pusztai, *Condensed Matter Physics*, 2013, **16**,.
27 B. Hess, H. Bekker, H. J. Berendsen, J. G. Fraaije *et al.*, *Journal of Computational Chemistry*, 1997, **18**, 1463–1472.
28 D. J. Evans and B. L. Holian, *J. Chem. Phys.*, 1985, **83**, 4069–4074.
29 M. Parrinello and A. Rahman, *J. Appl. Phys.*, 1981, **52**, 7182.
30 T. Lazaridis and M. Karplus, *J. Chem. Phys.*, 1996, **105**, 4294.
31 *This program can be downloaded from*, `http://gcm.upc.edu/en/members/luis-carlos/angula/ANGULA`, [Online; accessed 19-January-2016].
32 N. Veglio, F. Bermejo, L. Pardo, J. L. Tamarit and G. Cuello, *Physical Review E*, 2005, **72**, 031502.
33 L. Pardo, N. Veglio, F. Bermejo, J. L. Tamarit and G. Cuello, *Physical Review B*, 2005, **72**, 014206.
34 M. Rovira-Esteva, A. Murugan, L. Pardo, S. Busch, M. Ruiz-Martin, M.-S. Appavou, J. L. Tamarit, C. Smuda, T. Unruh, F. Bermejo *et al.*, *Physical Review B*, 2010, **81**, 092202.
35 I. Svishchev and P. Kusalik, *The Journal of Chemical Physics*, 1993, **99**, 3049–3058.
36 A. N. Dickey and M. J. Stevens, *Phys. Rev. E*, 2012, **86**, 051601.